

See discussions, stats, and author profiles for this publication at: <https://www.researchgate.net/publication/51692990>

# Cross-Linking Mechanisms of Arginine and Lysine with $\alpha,\beta$ -Dicarbonyl Compounds in Aqueous Solution

ARTICLE in THE JOURNAL OF PHYSICAL CHEMISTRY A · NOVEMBER 2011

Impact Factor: 2.69 · DOI: 10.1021/jp205558d · Source: PubMed

---

CITATIONS

5

READS

44

## 4 AUTHORS, INCLUDING:



Rasoul Nasiri

University of Brighton

23 PUBLICATIONS 89 CITATIONS

[SEE PROFILE](#)



Mansour Zahedi

Shahid Beheshti University

65 PUBLICATIONS 366 CITATIONS

[SEE PROFILE](#)



Ali A Moosavi-Movahedi

University of Tehran

520 PUBLICATIONS 5,454 CITATIONS

[SEE PROFILE](#)

# Cross-Linking Mechanisms of Arginine and Lysine with $\alpha,\beta$ -Dicarbonyl Compounds in Aqueous Solution

Rasoul Nasiri,<sup>†</sup> Martin J. Field,<sup>‡</sup> Mansour Zahedi,<sup>\*,†</sup> and Ali Akbar Moosavi-Movahedi<sup>§</sup>

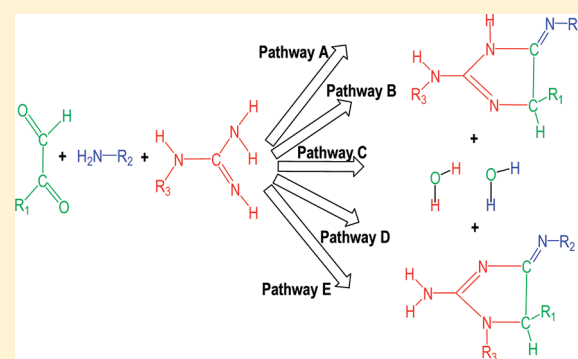
<sup>†</sup>Department of Chemistry, Faculty of Sciences, Shahid Beheshti University, Evin, 19839-63113 Tehran, Iran

<sup>‡</sup>Laboratoire de Dynamique Moléculaire, Institut de Biologie Structurale-Jean-Pierre Ebel, CNRS-CEA-UJF (UMRS075), Grenoble, France

<sup>§</sup>Institute of Biochemistry and Biophysics, University of Tehran, Tehran, Iran

Supporting Information

**ABSTRACT:** Cross-linking in proteins by  $\alpha,\beta$ -dicarbonyl compounds is one of the most damaging consequences of reactive carbonyl species in vivo and in foodstuffs. In this article we investigate computationally the cross-linking of glyoxal and methylglyoxal with lysine and arginine residues using density functional theory and the wB97XD dispersion-corrected functional. Five pathways, A–E, have been characterized. In pathways A and B, the reaction proceeds via formation of the Schiff base, aldimine, followed by addition of arginine. In contrast, in pathways C–E, direct addition of arginine to the dicarbonyl compounds occurs first, leading to a dihydroxyimidazolidine intermediate, which then reacts with lysine after dehydration and proton transfer reactions. The results reveal that pathways A, C, and E are competitive whereas reactions via pathways B and D are much less favorable. Inclusion of up to five explicit water molecules in the proton transfer and dehydration steps is found to lower the energy barriers in the feasible pathways by about 5–20 kcal/mol. Comparison of the mechanisms of methylglyoxal-derived imidazolium cross-linking (MODIC) and glyoxal-derived imidazolium cross-linking (GODIC) shows that the activation barriers are lower for GODIC than MODIC, in agreement with experimental observations.



## INTRODUCTION

Carbonyl stress<sup>1</sup> is an imbalance between the modification of proteins by reactive carbonyl species (RCSs) and their scavenging or detoxification. This disturbance contributes to numerous pathological and pathogenic conditions including renal insufficiency,<sup>2,3</sup> heart disease,<sup>4</sup> cancer,<sup>5</sup> Alzheimer's and Parkinson's diseases,<sup>6</sup> and homeostatic and other chronic disorders, such as diabetes, inflammation, and tumors.<sup>7</sup> RCSs, such as glyoxal (GO) and methylglyoxal (MGO) can be generated from the degradation of sugars,<sup>8–11</sup> lipids,<sup>12</sup> Schiff base intermediates and Amadori products<sup>13,14</sup> under physiological conditions. Significant quantities of  $\alpha$ -oxoaldehydes have been observed in vitro upon incubation of lysine and glucose<sup>15</sup> and also in vivo in human uremic plasma.<sup>16</sup> It has been postulated that these compounds are major causes of cross-linking both in plasma and within the cell.<sup>17</sup> Levels of GO and MGO in plasma are reported to be 215–230 nM,<sup>17b,c</sup> but these increase to 350–470 nM in diabetic subjects,<sup>17c,d</sup> to 400 nM in uremia,<sup>17a</sup> and to 760 nM in end-stage renal disease.<sup>17a</sup>

The structures of cross-links formed by the  $\alpha$ -oxoaldehydes with various amino acids and inhibitors have been elucidated experimentally,<sup>18–20</sup> with studies of the cross-linking of GO and MGO with lysine and arginine residues in proteins being

particularly extensive. Some of the products that are formed include carboxyethyl-lysine (CEL),<sup>20c</sup> methylglyoxal-lysine dimer (MOLD),<sup>20d</sup> carboxymethyl-lysine (CML),<sup>21</sup> carboxymethyl-arginine (CMA),<sup>22</sup> glyoxal-lysine dimer (GOLD),<sup>23</sup> glyoxal-derived imidazolium cross-link (GODIC), and methylglyoxal-derived imidazolium cross-link (MODIC).<sup>18,20a,b</sup> Of these, GODIC and MODIC have been recognized as being the most important in vitro and in vivo,<sup>18,20a,b</sup> although the molecular steps by which they arise are uncertain. One possible route that has been proposed is depicted in Scheme 1.<sup>18</sup> It involves the formation of an aldimine (Schiff base) by reaction of GO or MGO with lysine, followed by attack with the guanidino group on the side chain of an arginine residue. The reaction finishes by some rearrangement and proton transfer reactions that lead to the cross-linked product.

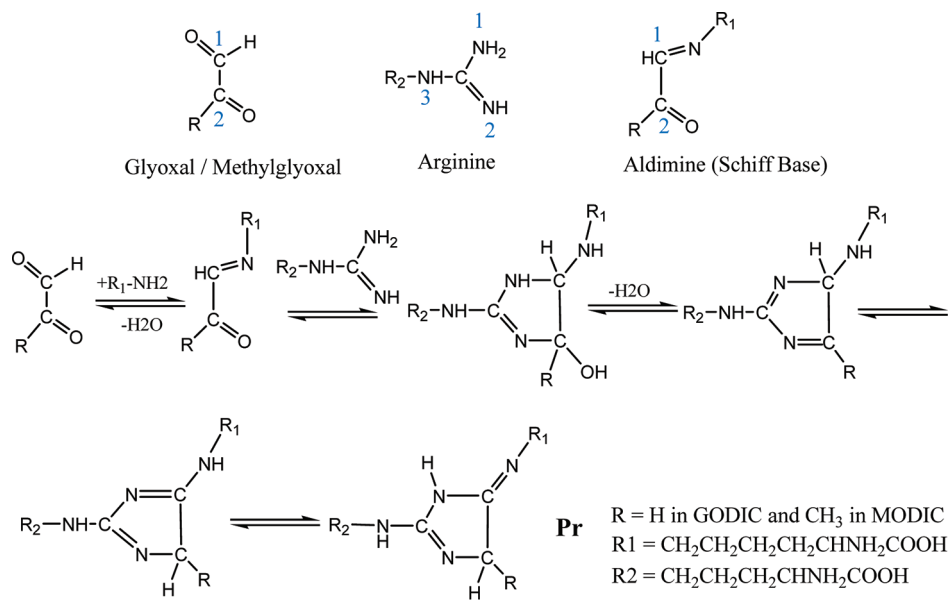
In the mechanism of Scheme 1, the final cross-links are formed uniquely through bonding of N<sub>1</sub> and N<sub>2</sub> of the arginine side chain (hereafter denoted exocyclic N<sup>δ</sup>) with the C<sub>1</sub> and C<sub>2</sub> from aldimine. The endocyclic homologues of GODIC or MODIC

**Received:** June 14, 2011

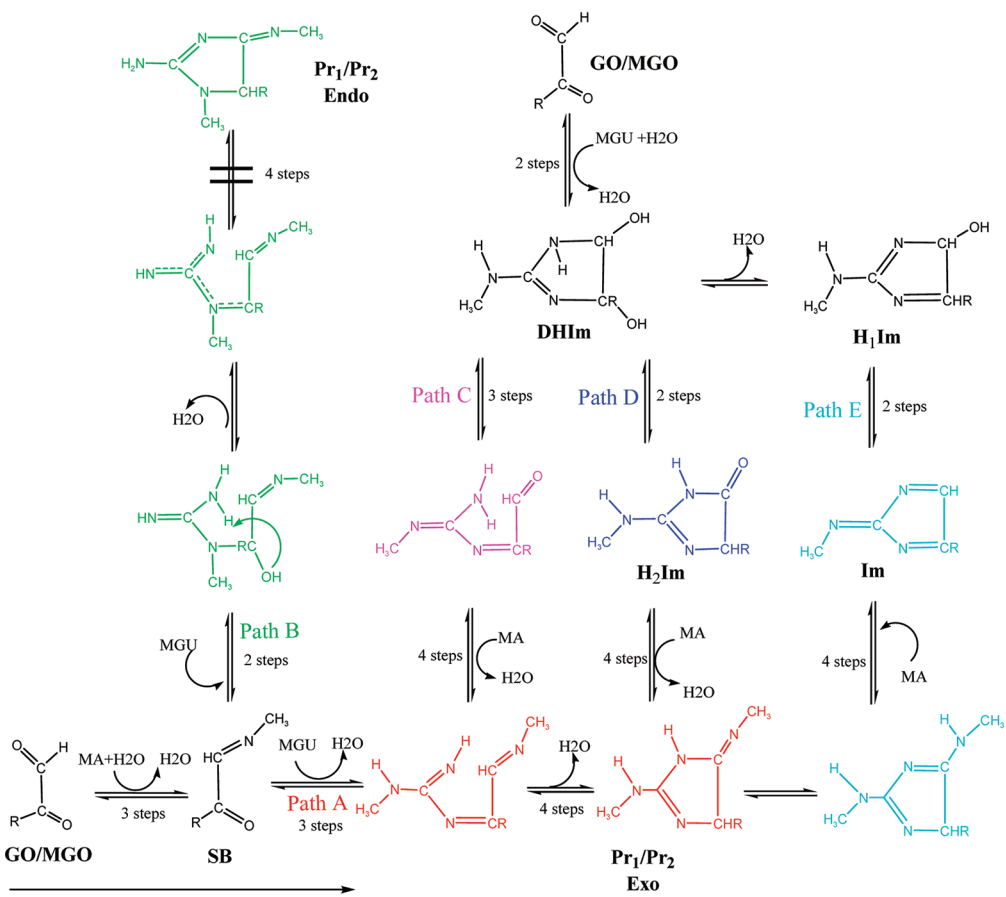
**Revised:** October 4, 2011

**Published:** October 05, 2011

**Scheme 1.** Proposed Mechanism for GODIC and MODIC Formation Derived from Cross-Linking of Dicarbonyl Compounds with Lysine and Arginine



**Scheme 2.** Overview of the Cross-Linking Process in Pathways A–E<sup>a</sup>



<sup>a</sup> Abbreviations used: GO, glyoxal; MGO, methylglyoxal; MA, methylamine; SB, Schiff base; MGU, methylguanidine; Im, imidazolone; DHIm, dihydroxyimidazolidine; H<sub>1</sub>Im, hydroxylimidazolone; H<sub>2</sub>IM, hydroimidazolone; Exo, exocyclic; Endo, endocyclic. Pr<sub>1</sub> is GODIC: R = H. Pr<sub>2</sub> is MODIC: R = CH<sub>3</sub>

**Table 1.** Relative Free Energies (kcal/mol)<sup>a</sup> for Stationary Points Involved in the Cross-Linking Reaction of GODIC and MODIC<sup>b</sup> in Solution<sup>c</sup>

	GODIC (MODIC)				
	A	B	C	D	E
GO (MGO)+MA+MGU	0.0	0.0	0.0	0.0	0.0
RC	2.9 (3.5)	2.9 (3.5)	0.3 (5.3)	0.3 (5.3)	0.3 (5.3)
TS1	9.0 (10.0)	9.0 (10.0)	1.0 (6.6)	1.0 (6.6)	1.0 (6.6)
Int1	-4.4 (-3.3)	-4.4 (-3.3)	-3.6 (2.6)	-3.6 (2.6)	-3.6 (2.6)
Int1'	-3.0 (0.7)	-3.0 (0.7)			
TS2	28.4 (33.1)	28.4 (33.1)	3.6 (10.7)	3.6 (10.7)	3.6 (10.7)
Int2	0.7 (2.1)	0.7 (2.1)	-11.5 (-5.0)	-11.5 (-5.0)	-11.5 (-5.0)
TS3	14.3 (17.2)	12.1 (15.3)	25.3 (30.8)	47.3 (46.2)	25.3 (30.8)
Int3	-5.1 (10.1)	3.2 (7.4)	-4.7 (-3.9)	-11.8 (-6.5)	-4.7 (-3.9)
TS4	13.7 (21.6)	26.5 (37.1)	6.3 (6.2) <sup>d</sup>	7.2 (15.2) <sup>d</sup>	6.3 (6.2) <sup>d</sup>
Int4	1.3 (8.6)	4.8 (21.2)	-1.1 (-1.7)	-32.6 (23.1)	0.5 (1.7)
TSS	31.3 (33.8)	35.7 (39.5)	22.9 (23.3) <sup>d</sup>	-27.1 (-20.7)	39.4 (10.9)
Int5	11.3 (11.7)	34.2 (35.7)	17.0 (17.7)	-27.3 (-24.5)	8.7 (9.6)
TS6	23.8 (21.7)	40.6 (41.0)	24.9 (28.9)	-3.3 (8.8)	14.2 (15.3)
Int6	23.7 (21.0)	13.5 (12.0)	10.7 (15.0)	-16.0 (-4.8)	6.8 (8.9)
TS7	24.5 (23.6)	10.2 (9.4) <sup>d</sup>	18.3 (20.4)	-1.0 (7.0)	7.0 (9.9) <sup>d</sup>
Int7	-8.0 (-6.8)	8.5 (8.3)	5.8 (10.2)	-29.3 (-19.9)	-8.2 (-7.5)
TS8	9.7 (13.7)	25.1 (26.4)	27.2 (33.0)	-14.6 (-5.9)	3.0 (-3.0) <sup>d</sup>
Int8	-32.5 (-24.0)	-28.9 (-20.6)	9.7 (13.0)		-8.5 (-8.8)
TS9	-14.6 (-6.0)		48.9 (50.8)		12.3 (16.2)
Int9			-8.2 (-6.8)		-30.9 (-21.5)
TS10			-1.2 (-1.0) <sup>d</sup>		-20.5 (-8.7)
Int10			-10.2 (-8.3)		
TS11			10.1 (14.0)		
Int11			-33.8 (-23.9)		
TS12			-14.6 (-5.9)		
Pr <sub>1</sub> (Pr <sub>2</sub> ) <sup>e</sup>	-25.0 (-15.6)	-32.1 (-25.0)	-25.0 (-15.6)	-25.0 (-15.6)	-26.1 (-17.3)

<sup>a</sup> Calculations were done at the CPCM/wB97XD/6-31+G\* level of theory. <sup>b</sup> All values in parentheses are for the MODIC cross-link. <sup>c</sup> Water has been used as the solvent. <sup>d</sup> These steps involved two water molecules. <sup>e</sup> Pr<sub>1</sub> and Pr<sub>2</sub> stand for GODIC and MODIC, respectively.

**Table 2.** Overall Activation Barriers<sup>a</sup> (kcal/mol at the CPCM/wB97XD/6-31++G\*\* Level of Theory) for Pathways A–E as a Function of the Number of Water Molecules

structure	GODIC (MODIC)				
	n <sup>b</sup> = 1	n = 2	n = 3	n = 4	n = 5
Pathway A					
TS2	26.0 (26.5)	19.4 (20.5)	18.7 (18.9)	15.4 (15.8)	18.4 (21.3)
TS2 <sup>d</sup>	30.0 (32.6)	22.7 (26.0)	18.1 (19.1)	16.7 (14.4)	21.2 (21.3)
TSS	27.2 (29.5)	25.7 (26.1)	22.6 (29.7)	23.8 (30.1)	17.7 (24.5)
Pathway B					
TS6	36.8 (37.5)	34.6 (35.3)	35.1 (35.9)	36.2 (36.6)	36.7 (37.1)
Pathway C					
TS3	25.0 (26.6)	21.6 (22.6)	17.9 (20.8)	20.8 (24.8)	20.7 (24.9)
TS8	24.4 (27.6)	20.9 (25.3)	20.0 (24.1)	20.1 (25.9)	22.6 (26.7)
TS9	39.3 (44.9)	25.6 (31.1)	23.6 (24.5)	23.2 (24.2)	22.7 (26.0)
Pathway D					
TS3	54.3 (57.4)	ND <sup>c</sup>	47.2 (49.5)	45.6 (46.5)	ND <sup>c</sup>
Pathway E					
TS3	25.0 (26.6)	21.6 (22.6)	17.9 (20.8)	20.8 (24.8)	20.7 (24.9)
TSS	35.4 (36.8)	31.9 (32.9)	30.5 (31.3)	28.2 (28.9)	31.0 (30.9)

<sup>a</sup> Refined free energies were determined for steps that were found to have large free energy barriers at the wB97XD/6-31+G\* level of theory. <sup>b</sup> n is the number of added water molecules in the studied processes. <sup>c</sup> Not determined. <sup>d</sup> Following the comments of a reviewer, we also calculated the free energy of TS2 with respect to Int1'.

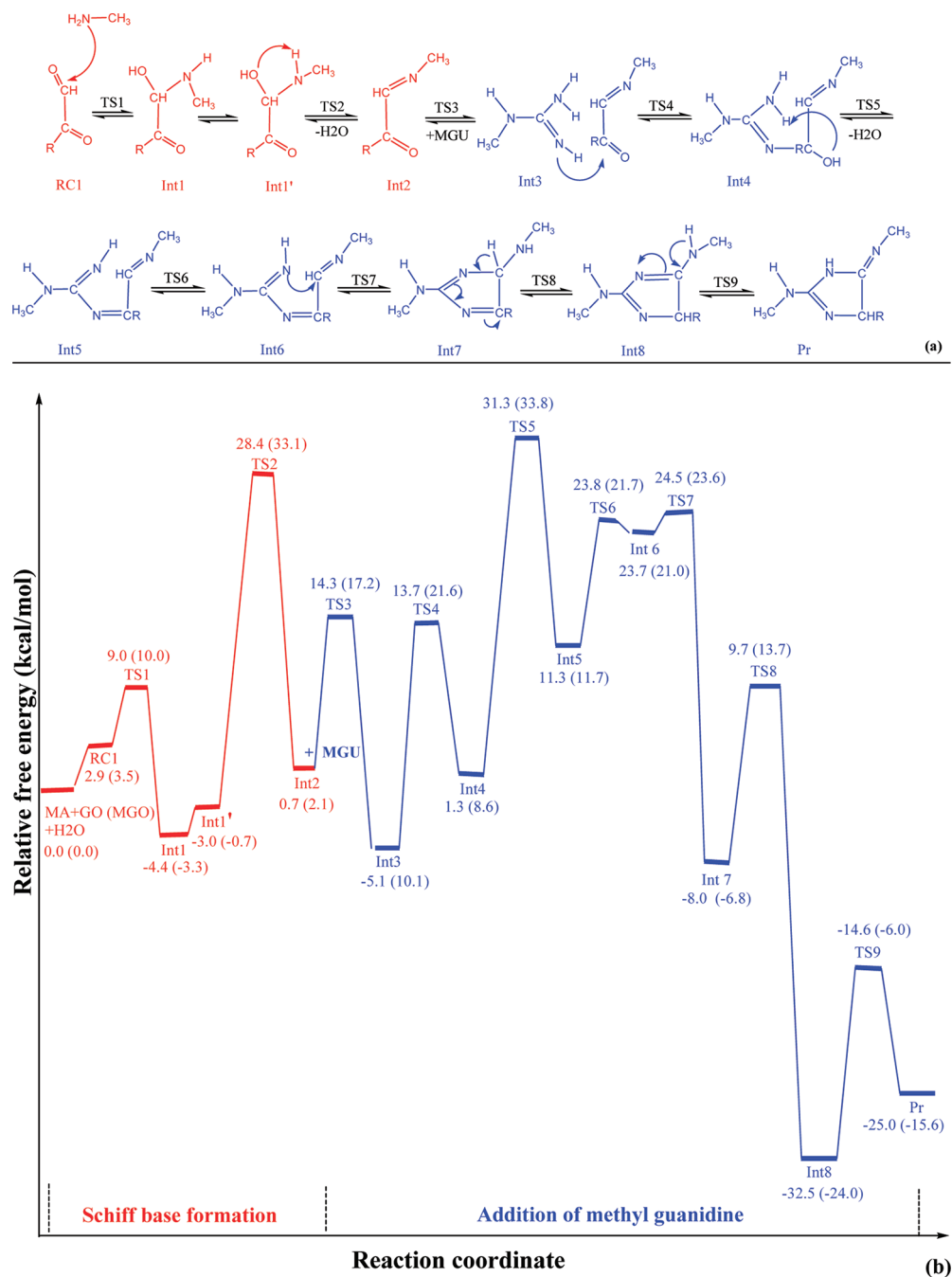


**Figure 1.** Pathway A: (a) scheme of cross-linking process; (b) free-energy profile for GODIC and MODIC (in parentheses) analogs in water calculated at the wB97XD/6-31+G\* level of theory.

formed with N<sub>3</sub> and either N<sub>1</sub> or N<sub>2</sub> have been shown not to occur.<sup>18</sup> In contrast, in other studies, it has been found that addition of the guanidino group to GO or MGO can occur through exocyclic and endocyclic N<sup>δ</sup> atoms in the formation of dihydroxyimidazolidine.<sup>20,24</sup>

These uncertainties, together with the difficulty of elucidating the mechanism of cross-linking experimentally, led us to undertake a quantum chemical computational study of both GODIC and MODIC. We examined a number of mechanistic hypotheses, which are illustrated in Scheme 2. In addition to the suggestion that cross-linking occurs via addition of an arginine residue to the

Schiff base<sup>18</sup> (pathways A and B), we also investigated the possibility that arginine could attack GO and MGO directly (pathways C–E). Our overall goal was to clarify the detailed mechanisms of cross-linking and to shed light on which pathways favor the glycation process, both thermodynamically and kinetically.

In our studies, we relied principally on density functional theory (DFT) using the wB97XD functional. Methylamine (MA) and methylguanidine (MGU) were selected as models of lysine and arginine residues to avoid complications due to conformational flexibility and to reduce computational expense.

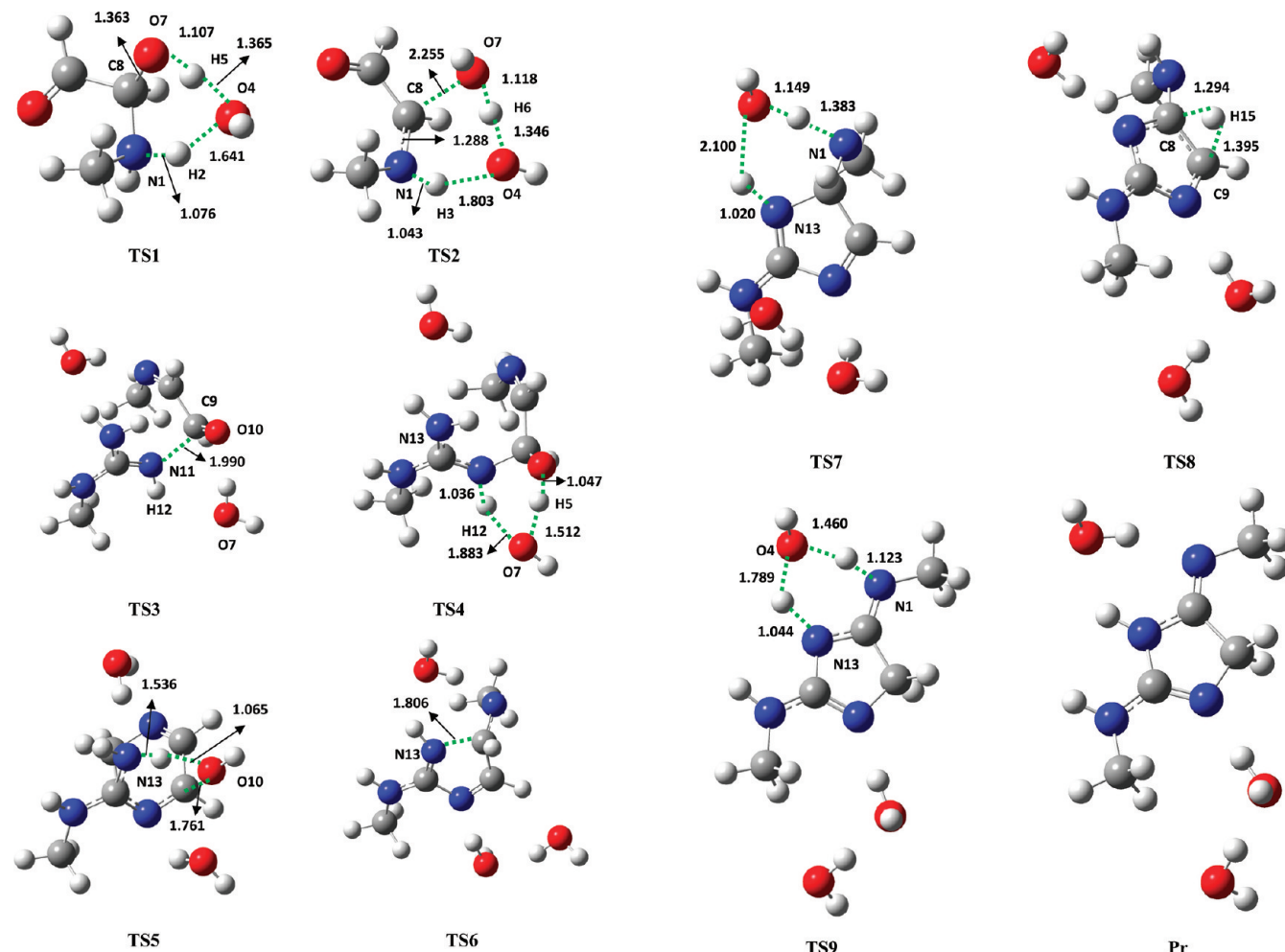


Figure 2. Structures of transition states and product from pathway A, including selected interatomic distances (Å).

Table 3. Comparison of Results Using DFT and CCSD(T) for Critical Barriers in Formation Mechanisms of GODIC in All Pathways

	Wb97xd/6-311++G**	CCSD(T)/6-311++G** <sup>a</sup>	Wb97xd/6-311++G**	CCSD(T)/6-311++G** <sup>a</sup>
TS2/pathway A	26	28.8	TS3/path C	26.4
TS2/pathway A <sup>b</sup>	19.4	20	TS9/path C	39.3
TSS/pathway A	27.2	25.6	TS3/path D	43.7
TS6/pathway B	36.8	35.3	TS3/path E	26.4
			TSS/path E	35.4
				32.7

<sup>a</sup> Single-point energies at CPCM/CCSD(T)/6-311++G\*\* levels were corrected by thermodynamic quantities obtained from full optimization at the CPCM/Wb97xd/6-311++G\*\* level of theory. <sup>b</sup> In the presence of two water molecules. All other results are in the presence of one water.

Solvent was represented both explicitly, by including up to five water molecules in the quantum chemical system, and implicitly, by using a solvent reaction field method.

## COMPUTATIONAL SCHEME

All calculations were done using a DFT method and the wB97XD functional.<sup>25</sup> The latter includes empirical dispersion and was designed to treat hydrogen bonding and van der Waals interactions more accurately than other functionals. The geometric structures for all reactant complexes (RC), product complexes (Pr), intermediates (Int), and transition states (TS),

were fully geometry optimized with the 6-31+G\* basis in the presence of usually one, but sometimes two, additional water molecules, which are often involved in the reaction process. The structures and energies of selected structures along the pathways were then rerefined with a variable number of waters (1–5) and the larger 6-311++G\*\* basis. The latter is an effective choice that gives an accurate description of hydrogen transfer reactions and hydrogen-bonded species, especially when water molecules are involved in the cross-linking process. Finally, some single point calculations were also carried out with a CCSD(T) method so as to provide a check on the DFT energies.

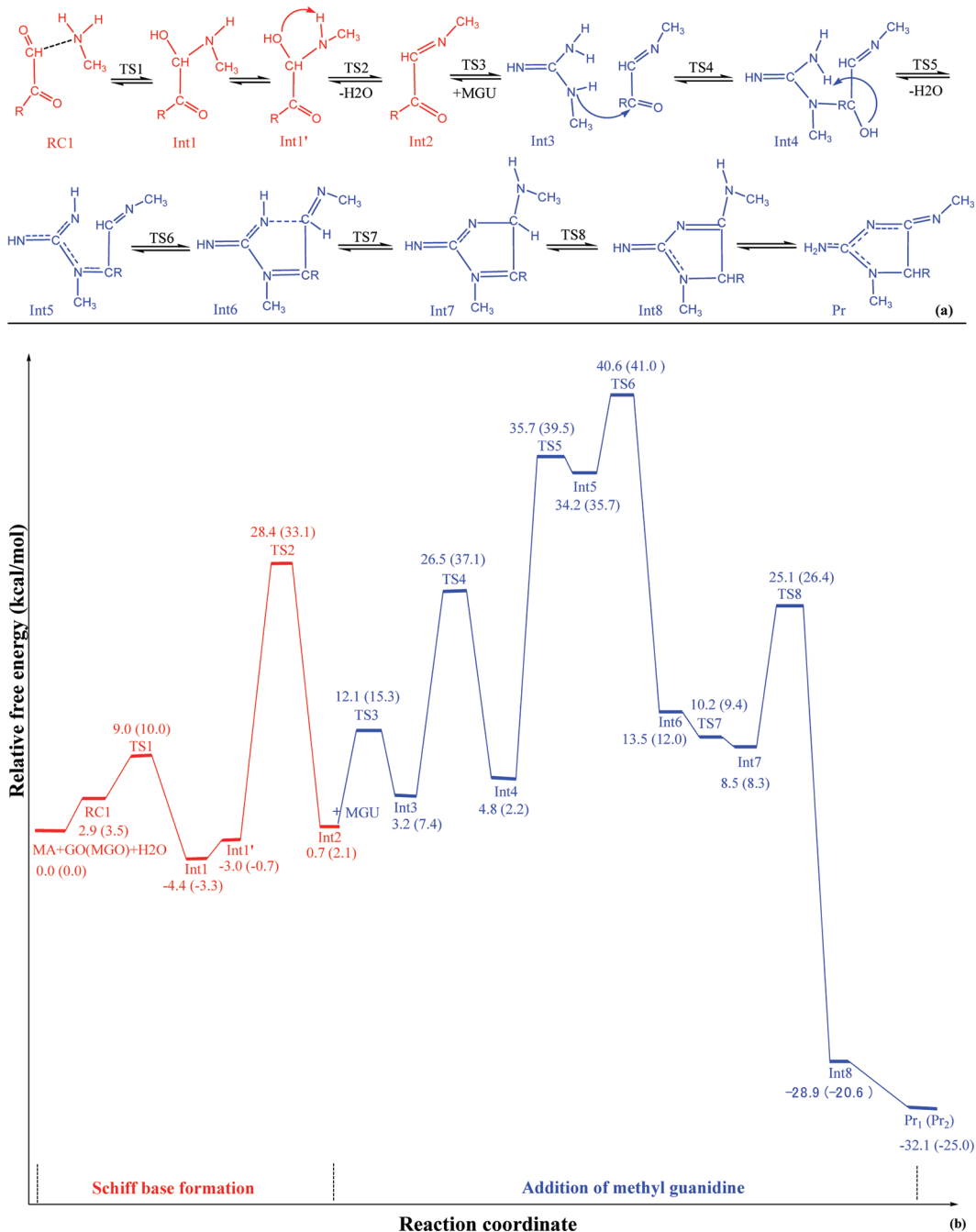


Figure 3. Pathway B. See Figure 1 for the definitions of (a) and (b).

When the reacting species were optimized with variable numbers of water molecules, differing starting points for the waters were considered. The ones given here are those with the lowest energies. Clearly, without a systematic conformational search, we cannot be sure that stationary points of lower energy do not exist. Nevertheless, we note that the structures that we report were almost invariably well separated in energy from alternatives, and that different starting points often led to identical structures, suggesting an insensitivity of the final structure to the initial ones.

Intrinsic reaction coordinate (IRC) calculations<sup>26</sup> were employed to ensure the identity of the reactants and products corresponding to each TS structure. Tables summarizing the IRC

results and values of imaginary frequencies of some stationary points are gathered in the Supporting Information.

To evaluate the effects of water, we employed a cluster-continuum model that made use of both a variable number of explicit water molecules and the implicit conductor-like-polarized continuum model (CPCM). The latter is based on a solvent reaction field method.

Vibrational analyses were performed on all optimized structures with the same functional and basis set as the corresponding geometry optimizations. All vibrational frequencies were left unscaled and used to obtain free energies at the experimental temperature of 323 K.<sup>18</sup> The free energy values for each step are computed using an ideal gas approximation with an effective

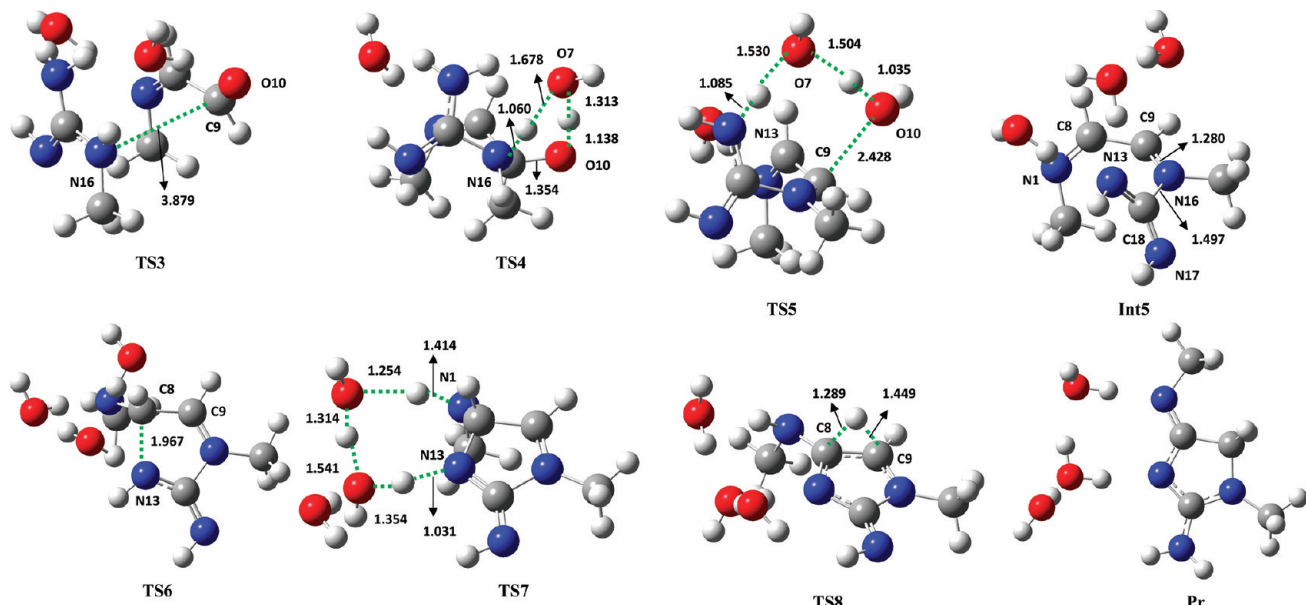


**Figure 4.** Structures of transition states, **Int5**, and product from pathway B (bond lengths in Å).

pressure of 1354 atm<sup>27</sup> to reduce translation entropy, because translational motions are suppressed in solution.

All calculations were performed using the Gaussian 09 software<sup>28</sup> and the Gauss View program for visualization.<sup>29</sup>

## RESULTS

This section explains in detail the structures and free energy profiles of the pathways, overviews of which are shown in Scheme 2. Each pathway was characterized for both GODIC and MODIC, and free energy values for all optimized structures in the solvent phase were calculated at the wB97XD/6-31+G\* level of theory. These values are presented in Table 1. In addition, certain critical, high-barrier steps along each pathway were recharacterized with the larger 6-311++G\*\* basis set, including a variable number of water molecules (1–5) near the reactive center. These refined values are presented in Table 2. The free energy profiles for each pathway are shown in Figures 1, 3, 5, 7, and 9, respectively, and some relevant structures in Figures 2, 4, 6, 8, and 10, respectively. A comparison of the DFT results with those of CCSD(T) calculations for all the critical barriers in the pathways of GODIC is given in Table 3.

**1. Pathway A: Schiff Base Formation and Exocyclic Addition of Methylguanidine.** This pathway corresponds to the mechanism of GODIC and MODIC proposed by Lederer and Klaiber.<sup>18</sup> In it, reaction of an  $\alpha,\beta$ -dicarbonyl compound with lysine produces a Schiff base, which is in turn attacked by arginine to give the cross-linking (Figures 1 and 2).

The mechanism starts with carbinolamine formation by nucleophilic attack of the methylamine group on the carbonyl carbon atom labeled as C<sub>8</sub> in Figure 2. This attack is performed via proton transfer from N<sub>1</sub> to O<sub>7</sub> and has a free energy barrier of 9 kcal/mol for the GODIC cross-link (Figure 1). In the six-membered ring TS, called **TS1** in Figure 2, the C<sub>8</sub>–N<sub>1</sub> bond is formed (1.52 Å) and the C<sub>8</sub>–O<sub>7</sub> bond has a length close to that of a single bond (1.36 Å). Schiff base formation is accomplished by dehydration of carbinolamine to yield a ketoimine. **Int1'** cannot be dehydrated directly, but it readily isomerizes to **Int1'** through two single bond rotations. Next, **Int1'** transforms to the

Schiff base, **Int2**, via a concerted proton transfer in which H<sub>3</sub> is transferred from N<sub>1</sub> to O<sub>4</sub> and H<sub>6</sub> from O<sub>4</sub> to O<sub>7</sub>. In the transition state for these proton transfers, **TS2** (Figure 2), the double bond between N<sub>1</sub> and C<sub>8</sub> is already formed. As can be seen from the reaction profile (Figure 1b), the activation free energy barrier for the dehydration step is high with a value, with respect to initial reactants, of 28.4 kcal/mol in solution. This is in agreement with high-level ab initio results on similar reactions<sup>30</sup> and with the results of a CCSD(T) calculation that gives a value of 28.8 kcal/mol. However, this barrier decreases substantially if the **TS2** structure is refined with extra water molecules around the reacting center (Table 2 along with the relevant structures in Figure S1, Supporting Information). The CCSD(T) value with two waters in the active center is 20.0 kcal/mol. Despite this reduction in barrier, comparison with the other steps in Schiff base formation shows that this remains the rate-limiting step, in agreement with experimental kinetic studies.<sup>31</sup>

**Int2** is a ketoimine compound that has two electrophilic centers and can react with MGU. Because of the existence of five acidic protons on the guanidino group, there are five different neutral methylguanidine tautomers (Scheme S1, Supporting Information). The most stable one (the E isomer) has been employed in this study, as shown by Norberg et al.<sup>32</sup> Addition of MGU to the Schiff base cannot occur unless N<sub>11</sub> from the guanidino group approaches the C<sub>9</sub> of aldimine (see Figure 2 for notation). The transition state for this process is **TS3** and the barrier is 13.6 kcal/mol. Because the NH group is more nucleophilic than NH<sub>2</sub> in neutral arginine, N<sub>11</sub> attacks C<sub>9</sub> of the Schiff base, once a reactive orientation has been achieved. There are two concomitant proton transfers and an overall free energy barrier of 18.8 kcal/mol. In the transition state structure for this process, **TS4**, a twisted six-membered ring is formed in which the proton is being transferred from N<sub>11</sub> to the water molecule, which in turn is already starting to transfer its proton to O<sub>10</sub>. The second dehydration occurs next to give **Int5**. The calculated activation barrier for this reaction, which passes by **TS5**, is very high and similar to the dehydration step in the first part of the pathway (**TS2** in Figure 1). However, as in that case,

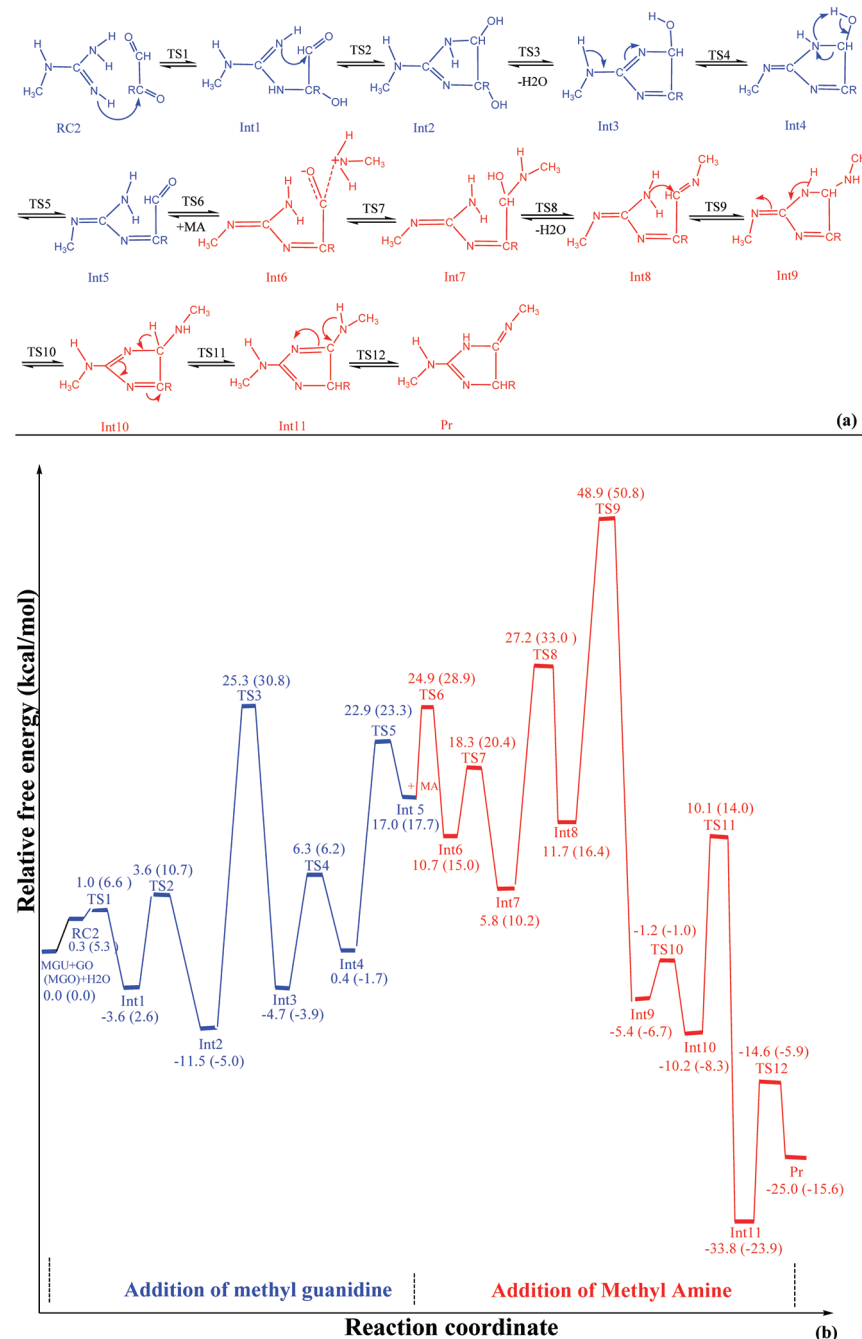


Figure 5. Pathway C. See Figure 1 for the definitions of (a) and (b).

the barrier significantly decreases with the addition of explicit waters around the reactive center (Table 2 along with Figure S2, Supporting Information).

For the subsequent step, the atoms N<sub>13</sub> and C<sub>8</sub> in Int5 need to approach each other. This is achieved through TS6 and leads to a high-energy intermediate, Int6, with a partially formed C<sub>8</sub>—N<sub>13</sub> bond. The C<sub>8</sub>—N<sub>13</sub> bond lengths in TS6 and Int6 are 1.81 and 1.58 Å, respectively. Int6 readily produces a five-membered heterocyclic structure, Int7, in which the C<sub>8</sub>—N<sub>13</sub> bond length is 1.46 Å. This reaction is highly exothermic, 31.7 kcal/mol, and occurs with a very low energy barrier of 0.8 kcal/mol. Its transition state, TS7, involves the concurrent transfer of two protons from N<sub>13</sub> to N<sub>1</sub>. Int7 itself undergoes a [1,5] H shift from

C<sub>8</sub> to C<sub>9</sub> to produce Int8, which is the most stable species along the reaction path. The reaction itself is highly exothermic (-24.5 kcal/mol) and occurs with a barrier of 17.7 kcal/mol (Figure 1). The last step of the mechanism is a concurrent proton transfer from N<sub>1</sub> to N<sub>13</sub> via a water molecule that produces the cross-linked product, Pr, which is less stable than Int8 by 7.5 kcal/mol in water (Figure 1).

The large decrease in free energy that we find in going from reactants to products would account for the irreversibility of the cross-linking process *in vivo* and in food.

**2. Pathway B: Schiff Base Formation and Endocyclic Addition of Methylguanidine.** Pathway B is identical to pathway A up to formation of the Schiff base but differs for the addition

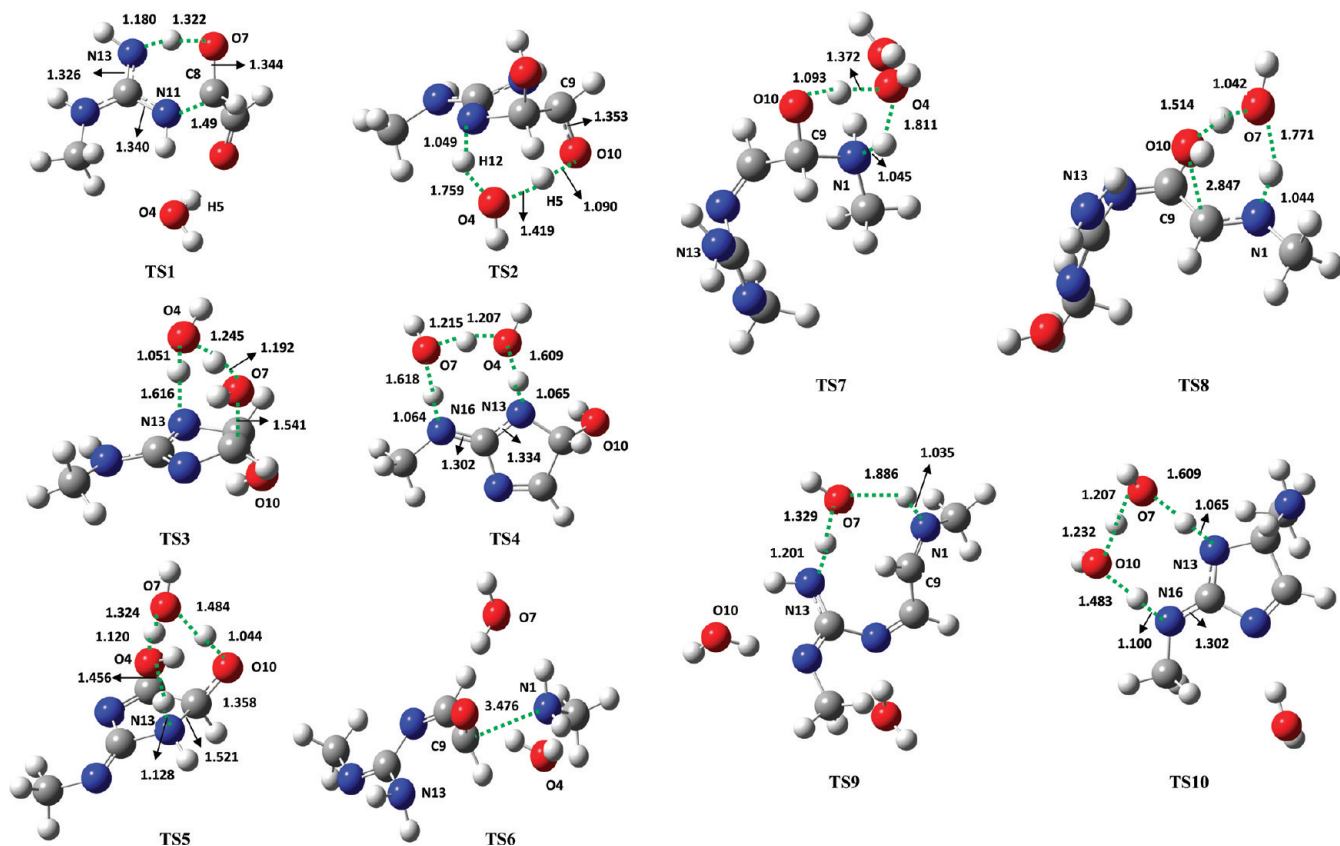


**Figure 6.** Structures of transition states from pathway C, with selected interatomic distances ( $\text{\AA}$ ).

of arginine, Figure 3. Pathway B was investigated to examine whether GODIC and MODIC formation could occur via the endocyclic  $\text{N}^{\delta}$  atoms of arginine residues. The best pathway that we found involved attack of the  $\text{N}_{16}$  of the guanidino group upon the aldimine  $\text{C}_9$ . This gave pathway B illustrated in Figure 3 in which MGU and the aldimine combine to give **Int3**, from which proton abstraction can occur. The formation of **Int3** from **Int2** is slightly thermodynamically unfavorable (+2.5 kcal/mol), whereas its equivalent in pathway A is exothermic by -5.8 kcal/mol (Figure 1). The subsequent step to **Int4**, via **TS4**, is also similar to that in pathway A although its activation barrier is about 5 kcal/mol higher.

The next step from **Int4** to **Int5** is dehydration with a large barrier of 30.9 kcal/mol, only slightly higher than the equivalent reaction in pathway A. A major difference between pathways A and B is the much higher energy of **Int5** in the latter, +34.2 kcal/mol, than in the former, +11.3 kcal/mol. Atomic population analysis of this intermediate, **Int5**, in the two pathways, indicates a positive, +0.2, charge on  $\text{N}_{16}$  in pathway B versus a negative, -0.4, charge in pathway A. In addition, the  $\text{N}_{16} - \text{C}_{17}$  bond length in the former is 1.5 Å, which is 0.1 Å longer than that in the latter (Figure 4). The next step, to form the five-membered ring in **Int6**, involves a relatively small barrier with respect to **Int5** and is highly exothermic.

We note that these last two steps are particularly difficult because higher level calculations in the presence of more water molecules only slightly reduces the barriers, as was the case in pathway A. Thus we can conclude that formation of GODIC or MODIC (Figure 3) through the endocyclic  $\text{N}^{\delta}$  is unlikely to occur. The free energy barrier for the next step, **Int6** to **Int7**, is

actually negative relative to **Int6** in solution. This is due to the zero-point vibrational and thermal corrections of the free energy, which lower the barrier by 3.8 kcal/mol. Without these corrections, the energy barrier is slightly positive at +0.6 kcal/mol. Such a phenomenon has been observed in other DFT studies in which low-barrier transition state structures were located.<sup>33–35</sup> The pathway terminates with two proton transfers that lead to the thermodynamically stable **Int8** and **Pr**. Although very stable, we were unable to locate a transition state, **TS9**, for formation of the product that has been reported in the literature.<sup>18</sup> The reaction itself requires a proton transfer from  $\text{N}_1$  to  $\text{N}_{17}$ .

**3. Pathway C: Ring-Opening of Dihydroxyimidazolidine and Addition of Methylamine.** The high reactivity of GO and MGO with arginine's guanidino group has been found experimentally.<sup>8</sup> We therefore decided to explore this possibility to see whether it is competitive with Schiff base formation in the cross-linking process (see the free energy profiles in Figures 1, 5, 7, and 9 for a comparison of pathways A, C, D, and E).<sup>8</sup>

The first two steps in the mechanism involve attack by the two guanidino  $\text{NH}_2$  groups on the carbonyl carbons of GO or MGO, along with a concomitant proton transfer. Both steps possess small free energy barriers and are thermodynamically favorable as **Int1** and **Int2** have free energies relative to reactants of -3.6 and -11.5 kcal/mol, respectively. The second proton transfer from  $\text{N}_{11}$  to  $\text{O}_{10}$  is achieved via an unstrained 7-membered ring transition state, **TS2** (Figure 6), with the assistance of a water molecule. The next step consists of a dehydration reaction, which is endothermic ( $\Delta G = +6.8$  kcal/mol) and has a very high barrier (**TS3**;  $\Delta G^{\ddagger} = 36.8$  kcal/mol), although inclusion of extra waters reduces this value substantially (Table 2 and Figure S3, Supporting

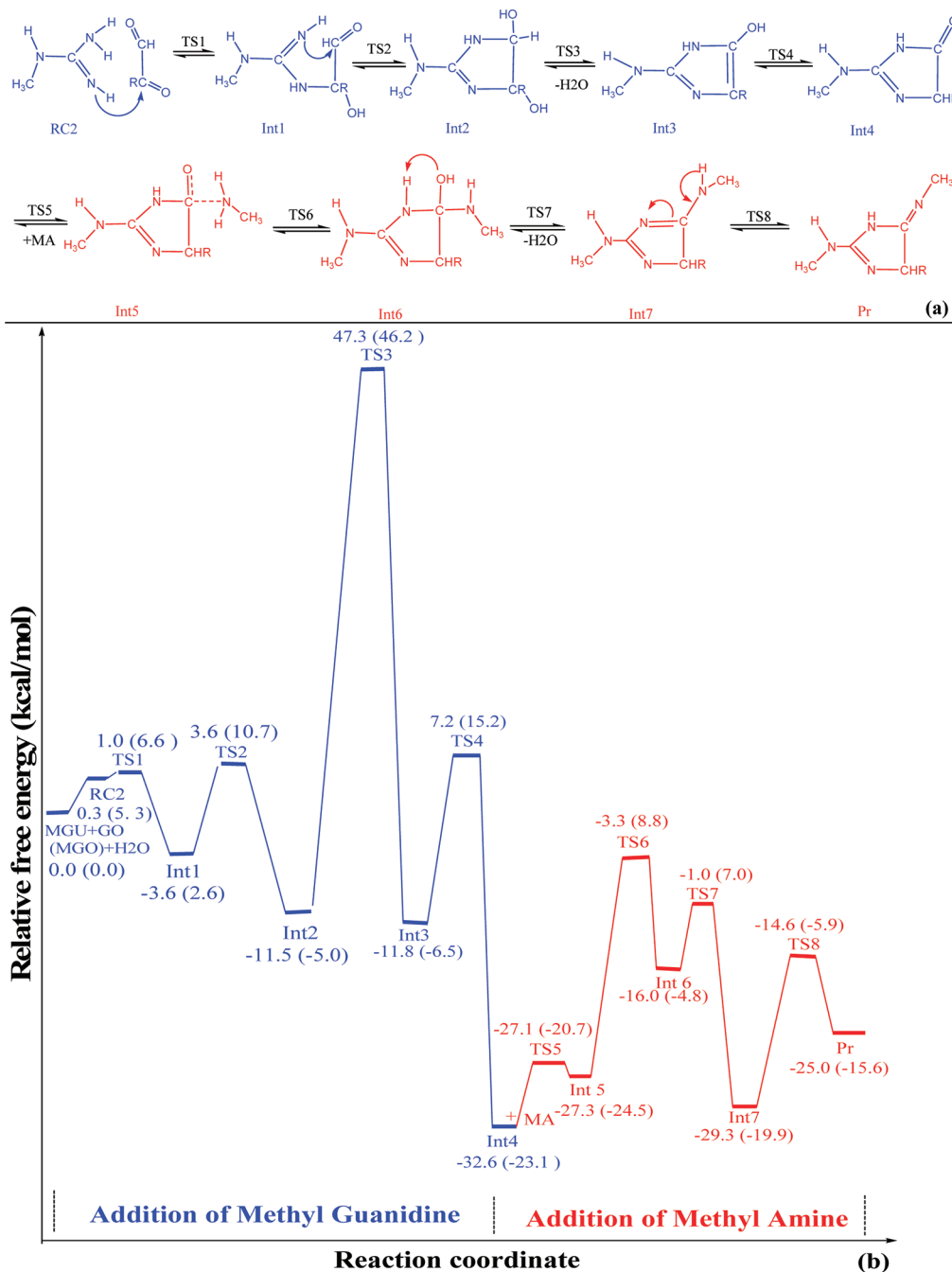


Figure 7. Pathway D. See Figure 1 for the definitions of (a) and (b).

Information). Dehydration is followed by a proton transfer from endocyclic N<sub>16</sub> to exocyclic N<sub>13</sub> which takes place concurrently through two water molecules (TS4 in Figure 6). Deprotonation of O<sub>10</sub> and protonation of N<sub>13</sub> then causes an imidazolone ring-opening in Int4 to give Int5 with an activation barrier of 22.5 kcal/mol.

Int5 possesses the electrophilic center, C<sub>9</sub>, which means that addition of MA occurs easily, via TS6, to form the zwitterionic Int6 (Figure 6). This subsequently undergoes a proton transfer from N<sub>1</sub> to O<sub>10</sub> to form the carbinolamine, Int7. Both these reactions are downhill processes ( $\Delta G = -6.3$  and  $-4.9$  kcal/mol, respectively) with relatively small barriers ( $\Delta G^\ddagger = 7.9$  and  $7.6$  kcal/mol, respectively). After this, dehydration follows with a significant activation barrier of 21.4 kcal/mol to give Int8. Once

this is formed, ring closure occurs by attack of N<sub>13</sub> on C<sub>9</sub> with the assistance of a water molecule in the proton transfers (TS9 in Figure 6). This reaction is very exothermic,  $-16.1$  kcal/mol, but is also rate-limiting as it has a large barrier of 37.2 kcal/mol. However, the barrier decreases dramatically to 22.7 kcal/mol when five water molecules are included in the reactive center (Table 2 and Figure S5, Supporting Information). The subsequent steps are identical to those described for pathway A and involve proton shifts through the intermediates, Int10 and Int11, before leading to product.

**4. Pathway D: Dehydration of Dihydroxyimidazolidine Obtained from Methylguanidine and  $\alpha,\beta$ -Dicarbonyl Compounds.** All stationary points up to Int2 are similar to those of

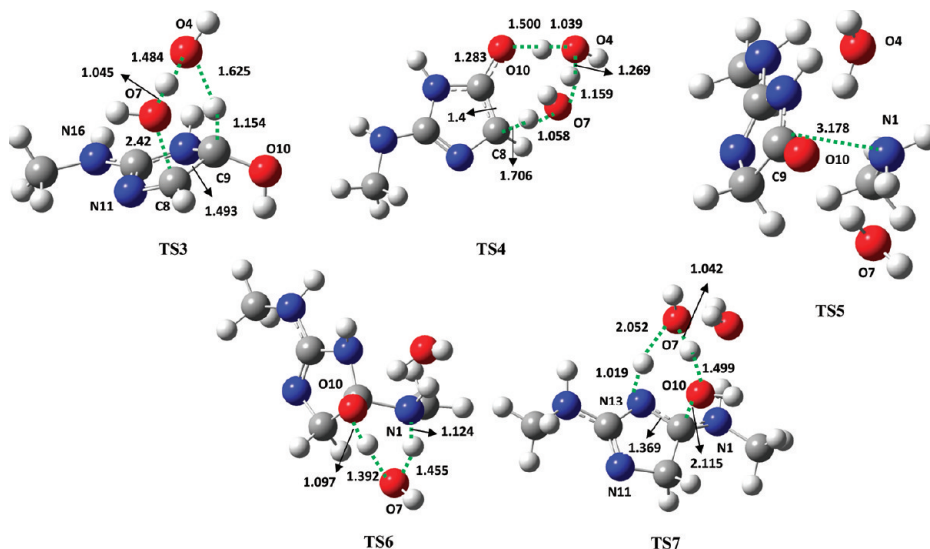


**Figure 8.** Structures of transition states from pathway D. Selected interatomic distances are given in Å.

pathway C. After this, the dehydration reaction occurs through a six-membered ring transition state, **TS3**, in which the proton on  $\text{C}_9$  is transferred to the hydroxyl group on  $\text{C}_8$  via one water molecule. This transition state corresponds to the highest barrier of the cross-linking process. Adding more water molecules does not lower the barrier significantly (Table 2), which indicates that water itself cannot facilitate this reaction. This is in accord with the experimental results of Glomb and Lang<sup>24b</sup> who showed that conversion of **Int2** (DHIm) to **Int4** (H2Im) can only occur under acidic conditions and elevated temperatures of 95 °C in vitro (see Scheme 2 for notation and ref 24b). Dehydration is followed by an enol–keto tautomerization in which a proton in **Int3** is shuttled from  $\text{O}_{10}$  to  $\text{C}_8$  to give **Int4**. This reaction is highly exothermic, −20.8 kcal/mol, and occurs via **TS4** (Figure 8) with a barrier of 19.0 kcal/mol (Figure 7). In the second step of the pathway, addition of MA occurs easily. This necessitates the formation of a reactive complex, **Int5**, in which  $\text{N}_1$  approaches  $\text{C}_9$ , and occurs via **TS5** (Figure 8) with a barrier of 5.5 kcal/mol. The next steps consist of a proton transfer to form **Int6** ( $\Delta G^\ddagger = 24.0$  kcal/mol and  $\Delta G = +11.3$  kcal/mol), followed by dehydration of carbinolamine ( $\Delta G^\ddagger = 15$  kcal/mol and  $\Delta G = -13.3$  kcal/mol), thereby generating the final product.

It can be concluded from these results that the conversion of dihydroxyimidazolidine to hydroimidazolone is not feasible, in agreement with experimental results<sup>24b</sup>. Interestingly, Cotham et al.<sup>8b</sup> have shown the essential catalytic role that enzymes play in formation of hydroimidazolone compounds from the reaction of GO with arginine residues close to the active site of ribonuclease (RNase). Ahmed et al.<sup>8a</sup> also saw similar behavior when studying the glycation of human serum albumin by MGO and GO.

**5. Pathway E: Successive Dehydration Reactions of Dihydroxyimidazolidine (DHIm).** Additional searches of the potential energy surface indicated that another mechanism was possible in which a second dehydration reaction occurs after addition of methylguanine but before addition of methylamine. This contrasts with the other pathways for which a single dehydration step accompanies each addition (Figure 9; compare with Figures 1, 3, 5, and 7). In this pathway, E, **Int4** in pathway C follows another route in which the hydrogen of  $\text{N}_{13}$  is transferred to  $\text{O}_{10}$  to give the dehydrated imidazolone **Int5**. This reaction is

endothermic with **Int5** 8.2 kcal/mol higher in energy than **Int4** and also a high barrier of 38.9 kcal/mol (**TS5** above **Int4**). Inclusion of more water molecules produces less strained transition states than **TS5** (Figure S6, Supporting Information, and Table 2) and the activation barrier decreases to 28.2 kcal/mol. In the latter transition state structures, two water molecules act as a proton transfer bridge and another stabilizes the structure via formation of a hydrogen bond. Addition of MA to the imidazolone **Int5** occurs easily because the barrier for this downhill reaction is calculated to be 5.5 kcal/mol (**TS6** in Figure 10). This step leads to a zwitterionic species in solution, which is further stabilized after an additional proton transfer (**TS7**;  $\Delta G = -15.0$  kcal/mol and  $\Delta G^\ddagger = 0.2$  kcal/mol). Two water molecules assist in this reaction. The subsequent steps are similar to those of pathway C.

**6. Mechanisms with Alternative Protonation States.** In this section we briefly consider what effect alternative protonation states would have on our reaction schemes. In the calculations of pathways A and B, we employed the deprotonated forms of reactants, intermediates, and products for Schiff base formation. The latter is also possible under acidic conditions in which the relevant species are protonated. This was considered by Hall and Smith in their study of the reaction of formaldehyde with methylamine.<sup>30</sup> We performed calculations under acidic conditions for the reaction of GO/MGO with MA, and our results are shown in Figures S7 and S8, Supporting Information.

Overall, the differences in energetics between the acidic and neutral pathways are relatively small. The results show that the protonated structures are lower in energy than their neutral analogues (compare Figures 1 and S7, Supporting Information) and that the barrier of the rate limiting step is slightly smaller than in the neutral pathway. These findings imply that Schiff base formation under acidic conditions is slightly more favorable kinetically and thermodynamically than under neutral ones. However, it is worth noting that deprotonation of the protonated Schiff base involves a large positive free energy (last step in Figure S7, Supporting Information).

In contrast to the first step, the cross-linking process of the second step is unlikely to proceed with the protonated form of aldimine, because the addition reaction of MGU to aldimine requires the transfer of a proton from the  $\text{NH}_2$  group in MGU to

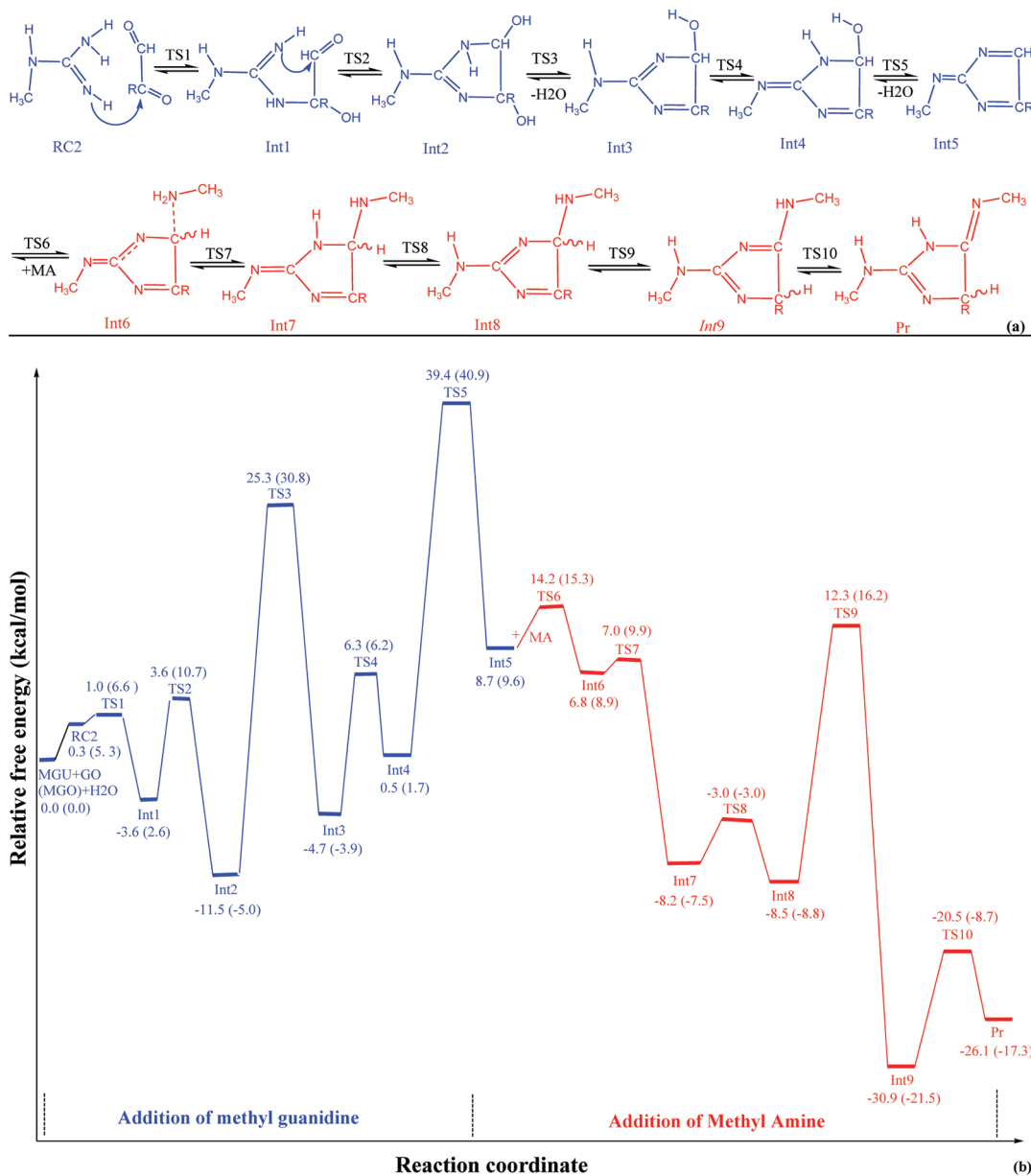


Figure 9. Reaction Pathway E. See Figure 1 for definition of (a) and (b).

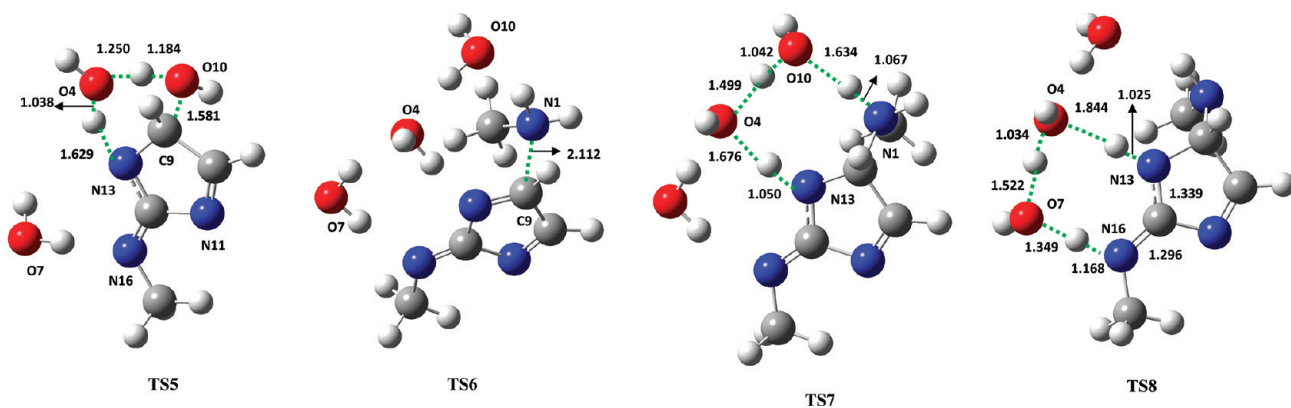


Figure 10. Structures of transition states from pathway E. Selected interatomic distances are given in Å.

the aldimine nitrogen. This is likely to be prevented if the nitrogen is already protonated. These explanations are in good agreement with experimental evidence that indicates that GODIC and MODIC are labile under conventional acid conditions.<sup>20b</sup> Similar results were obtained by Ahmed et al.<sup>20l</sup> who showed that hydroimidazolones ( $H_2Im$  in Scheme 2) were decomposed during acid hydrolysis. Therefore, it can be concluded that cross-link formation via pathways A and B cannot occur with protonated reactants and intermediates.

Equally, pathways C–E appear less likely under acidic conditions for two reasons. First, experiments have shown that DHIm, which is an important intermediate in these pathways, is unstable in acidic conditions. Second, if  $\alpha,\beta$ -dicarbonyl compounds are protonated, addition of MGU will not proceed for similar reasons to those mentioned for addition of MGU to a protonated Schiff base.

**7. Mechanisms of MODIC versus GODIC.** A comparison of the mechanisms of cross-linking in all pathways (Figures 1, 3, 5, 7, and 9) reveals that the MODIC activation barriers are larger than the equivalent GODIC values, especially when water molecules are involved in the processes and the barriers in the rate-limiting steps are computed at a higher level (Table 2). These findings are consistent with the observations of Lederer and Klaiber<sup>18</sup> who noted that the rate of GODIC is higher than that of MODIC. This is due, most probably, to the steric and electron-donating effects of the methyl group in MGO. In addition, MODIC is less thermodynamically favorable than GODIC, because the global reaction free energy change increases from  $-25.0$  to  $-15.6$  kcal/mol (see the initial and final free energies in Figure 1, 3, 5, 7, and 9). It is interesting to note that despite this, the overall mechanisms remain similar for GO and MGO and that the nature of the  $\alpha,\beta$ -dicarbonyl compounds did not influence the identity of the rate-limiting steps in any of the pathways.

## CONCLUSIONS

The cross-linking process of lysine and arginine residues with glyoxal and methylglyoxal has been studied using computational DFT techniques. Of the five possible mechanisms that we studied, pathways A and C were found to be the most probable ones in aqueous solution with pathway E a close third. Initial free energy values in these pathways show that guanidino groups are more reactive than amino functions in scavenging  $\alpha,\beta$ -dicarbonyl compounds, in agreement with some experimental studies.<sup>8c,d</sup> Pathways B and D involve very high free energy barriers, confirming that formation of GODIC and MODIC is not possible through endocyclic  $N^{\delta}$  (pathway B) and that the dehydration reaction of dihydroxyimidazolidine (DHIm) that follows formation of hydroimidazolone ( $H_2Im$ ) is kinetically unfavorable in water solution (pathway D). Overall our results are in good agreement with experimental conclusions.<sup>18,24b</sup>

This study provides new insights on how formation of cross-links by reactive carbonyl species occurs and should be useful in better understanding cross-linking processes *in vivo* and in food systems. We aim to extend this work in the future by studying the dynamics of these processes in protein with more complete molecular models of the reacting species and to investigate additional types of cross-linking reaction.

## ASSOCIATED CONTENT

**Supporting Information.** Full ref 28. Figures S<sub>1</sub>–S<sub>9</sub> (transition state structures, free energy profiles, stationary point

structures), Scheme S<sub>1</sub> (guanidine structures), Tables S<sub>1</sub>–S<sub>3</sub> (free energies, enthalpies and entropies, BSSE values), Cartesian coordinates, and Gibbs free energies for selected stationary points. This material is available free of charge via the Internet at <http://pubs.acs.org>.

## AUTHOR INFORMATION

### Corresponding Author

\*E-mail: M.Z., m-zahedi@sbu.ac.ir. Tel: +98 21 22401765/29902889. Fax: +98 21 22401765/22431663.

## ACKNOWLEDGMENT

The financial support of Research Council of Shahid Beheshti University is gratefully acknowledged.

## REFERENCES

- (1) Thomas, M. C.; Forbes, J. *Maillard Reaction: Interface between Aging, Nutrition and Metabolism*; RSC Publications: London, 2010.
- (2) Lim, J. S.; Mietus-Snyder, M.; Valente, A.; Schwarz, J.-M.; Lustig, R. H. *Nature* **2010**, *7*, 251–264.
- (3) Bierhaus, A.; Schiekofer, S.; Schwaninger, M.; Andrassy, M.; Humpert, P. M.; Chen, J.; Hong, M.; Luther, T.; Henle, T.; Klöting, I.; Morcos, M.; Hofmann, M.; Tritschler, H.; Weigle, B.; Kasper, M.; Smith, M.; Perry, G.; Schmidt, A. M.; Stern, D. M.; Häring, H. U.; Schleicher, E.; Nawroth, P. P. *Diabetes* **2001**, *50*, 2792–2808.
- (4) Hartog, J. W.; Voors, A. A.; Bakker, S. J.; Smit, A. J.; van Veldhuisen, D. J. *Eur J. Heart. Fail.* **2007**, *9*, 1146–1155.
- (5) (a) Tesařová, P.; Kalousová, M.; Jáchymová, M.; Mestek, O.; Petruzelka, L.; Zima, T. *Cancer Investigation* **2007**, *25*, 720–725. (b) Jing, R.; Cui, M.; Wang, J.; Wang, H. *Neoplasma* **2010**, *57*, 55–61.
- (6) (a) Grillo, M. A.; Colombatto, S. *Amino Acids* **2008**, *35*, 29–36. (b) Takeuchi, M.; Kikuchi, S.; Sazaki, N.; Suzuki, T.; Watai, T.; Iwaki, M.; Bucala, R.; Yamagishi, S. *Curr. Alzheimer. Res.* **2004**, *1*, 39–46.
- (7) Bucciarelli, L. G.; Wendt, T.; Rong, ; Lalla, E.; Hofmann, M. A.; Goova, M. T.; Taguchi, A.; Yan, S.; Yan, S. D.; Stern, D. M.; Schmidt, A. M. *Cell. Mol. Life. Sci.* **2002**, *59*, 1117–1128.
- (8) (a) Ahmed, N.; Argirov, O. K.; Minhas, H. S.; Cordeiro, C. A. A.; Thornalley, P. J. *Biochem. J.* **2002**, *364*, 1–14. (b) Cotham, W. E.; Metz, T. O.; Ferguson, P. L.; Brock, J. W. C.; Hinton, D. J. S.; Thorpe, S. R.; Baynes, J. W.; Ames, J. M. *Mol. Cell. Proteomics* **2004**, *3*, 1145–1153. (c) Brock, J. W. C.; Cotham, W. E.; Thorpe, S. R.; Baynes, J. W.; Ames, J. M. *J. Mass Spectrom.* **2007**, *42*, 89–100. (d) Thornalley, P. J. *Ann. N. Y. Acad. Sci* **2005**, *1043*, 111–117.
- (9) Thornalley, P. J.; Wolff, S. P.; Crabbe, J.; Stern, A. *Biochim. Biophys. Chim. Acta* **1984**, *797*, 276.
- (10) Wolff, S. P.; Dean, R. T. *Biochem. J.* **1987**, *245*, 243–250.
- (11) Wells-Knecht, K. J.; Zyzak, D. V.; Litchfield, J. E.; Thorpe, S. R.; Baynes, J. W. *Biochemistry* **1995**, *21* (34), 3702–9.
- (12) Beisswenger, P. J.; Szwerdgold, B. S.; Yeo, K. T. *Clin. Lab. Med.* **2001**, *21*, 53–78.
- (13) Zyzak, D. V.; Richardson, J. M.; Thorpe, S. R.; Baynes, J. W. *Arch. Biochem. Biophys.* **1995**, *316*, 547.
- (14) Martins, S. I.; Marcelis, A. T.; van Boekel, M. A. *Carbohydr. Res.* **2003**, *338*, 1651.
- (15) Gobert, J.; Glomb, M. A. *J. Agric. Food. Chem.* **2009**, *57*, 8591–8597.
- (16) Odani, H.; Shinzato, T.; Matsumoto, Y.; Usami, J.; Maeda, K. *Biochem. Biophys. Res. Commun.* **1999**, *256*, 89–93.
- (17) (a) Thornalley, P. J. *Biochem. J.* **1990**, *269*, 1–11. (b) Agalou, S.; Karachalias, N.; Thornalley, P. J.; Tucker, B.; Dawnay, A. B. *International Congress Series 1245. Excerpta Medica*; Elsevier: Amsterdam, The Netherlands, 2002; pp 181–182. (c) Lapolla, A.; Flamini, R.; Tonus, T.; Fedele, D.; Senesi, A.; Reitano, R.; Marotta, E.; Pace, G.; Seraglia, R.; Traldi, P. *Rapid Commun. Mass. Spectrom.* **2003**, *17*, 876–878. (d) Lapolla, A.; Flamini, R.; Dalla Vedova, A.; Senesi, A.; Reitano, R.;

- Fedele, D.; Bassi, E.; Seraglia, R.; Traldi, P. *Clin. Chem. Lab. Med.* **2003**, *41*, 1166–1173.
- (18) Lederer, M. O.; Klaiber, R. G. *Bioorg. Med. Chem.* **1999**, *7*, 2499–2507.
- (19) (a) Biemel, K. M.; Reihl, O.; Conrad, J.; Lederer, M. O. *J. Biol. Chem.* **2001**, *276*, 23405. (b) Chetyrkin, S. V.; Zhang, W.; Hudson, B. G.; Serianni, A. S.; Voziany, P. A. *Biochemistry* **2008**, *47*, 997–1006.
- (20) (a) Sell, D. R.; Biemel, K. M.; Reihl, O.; Lederer, M. O.; Strauch, C. M.; Monnier, V. M. *J. Biol. Chem.* **2005**, *280*, 12310. (b) Biemel, K. M.; Friedl, D. A.; Lederer, M. O. *J. Biol. Chem.* **2002**, *277*, 24907–24915. (c) Ahmed, M. U.; Brinkmann Frye, E.; Degenhardt, T. P.; Thorpe, S. R.; Baynes, J. W. *Biochem. J.* **1997**, *324*, 565. (d) Brinkmann, E.; Wells-Knecht, K. J.; Thorpe, S. R.; Baynes, J. W. *J. Chem. Soc. Perkin Trans. I* **1995**, *2817*. (e) Brinkmann, E.; Degenhardt, T. P.; Thorpe, S. R.; Baynes, J. W. *J. Biol. Chem.* **1998**, *273*, 18714. (f) Nagaraj, R. H.; Shipanova, I. N.; Faust, F. M. *J. Biol. Chem.* **1996**, *271*, 19338. (g) Shipanova, I. N.; Glomb, M. A.; Nagaraj, R. H. *Arch. Biochem. Biophys.* **1997**, *344*, 29. (h) Gomes, R.; Sousa Silva, M.; Quintas, A.; Cordeiro, C.; Freire, A.; Pereira, P.; Martins, A.; Monteiro, E.; Barroso, E.; Ponces Freire, A. *Biochem. J.* **2005**, *385*, 339. (i) van Heijst, J. W.; Niessen, H. W.; Hoekman, K.; Schalkwijk, C. G. *Ann. N. Y. Acad. Sci.* **2005**, *1043*, 725. (j) Oya, T.; Hattori, N.; Mizuno, Y.; Miyata, S.; Maeda, S.; Osawa, T.; Uchida, K. *J. Biol. Chem.* **1999**, *274*, 18492. (k) Lo, T. W. C.; Westwood, M. E.; McLellan, A. C.; Selwood, T.; Thornalley, P. J. *J. Biol. Chem.* **1994**, *169*, 32299. (l) Ahmed, N.; Argirov, O. K.; Minhas, H. S.; Cordeiro, C. A. A.; Thornalley, P. J. *Biochem. J.* **2002**, *364*, 1. (m) Nakayama, T.; Hayase, F.; Kato, H. *Agric. Biol. Chem.* **1980**, *44*, 1201. (n) Hayase, F.; Nagaraj, R. H.; Miyata, S.; Njorogege, G.; Monnier, V. M. *J. Biol. Chem.* **1989**, *264*, 3758. (o) Jono, T.; Nagai, R.; Lin, X.; Ahmed, N.; Thornalley, P. G.; Takeya, M.; Horiuchi, S. *J. Biochem.* **2004**, *136*, 351. (p) Nagaraj, R. H.; Sady, C. *FEBS Lett.* **1996**, *382*, 234. (q) Skovsted, I. C.; Christensen, M.; Breinholt, J.; Mortensen, S. B. *Cell.Mol. Biol.* **1998**, *44*, 1159. (r) Niwa, T.; Katsuzaki, T.; Ishizaki, Y.; Hayase, F.; Miyazaki, T.; Uematsu, T.; Tatemichi, N.; Takei, Y. *FEBS Lett.* **1997**, *407*, 297.
- (21) Reddy, S.; Bichler, J.; Wells-Knecht, K. J.; Thorpe, S. R.; Baynes, J. W. *Biochemistry* **1995**, *34*, 10872–10878.
- (22) (a) Iijima, K.; Murata, M.; Takahara, H.; Irie, S.; Fusimoto, D. *Biochem. J.* **2000**, *347*, 23. (b) Odani, H.; Iijima, K.; Nakata, M.; Miyata, S.; Kusunoki, H.; Yasuda, Y.; Hiki, Y.; Irie, S.; Maeda, K.; Fujimoto, D. *Biochem. Biophys. Res. Commun.* **2001**, *285*, 1232.
- (23) (a) Odani, H.; Shiznato, T.; Usami, J.; Matsumoto, Y.; Brinkmann Frye, E.; Baynes, J. W.; Maeda, K. *FEBS Lett.* **1998**, *427*, 381. (b) Chellan, P.; Nagaraj, R. H. *Arch. Biochem. Biophys.* **1999**, *368*, 98. (c) Wells-Knecht, K. J.; Brinkmann, E.; Baynes, J. W. *J. Org. Chem.* **1995**, *60*, 6246.
- (24) (a) Pfer, A.; Spanneberg, R.; Glomb, M. A. *J. Agric. Food Chem.* **2011**, *59*, 394–401. (b) Marcus, A.; Glomb, M. A.; Lang, G. *J. Agric. Food Chem.* **2001**, *49*, 1493–1501.
- (25) Chai, J. D.; Head-Gordon, M. *Phys. Chem. Chem. Phys.* **2008**, *10*, 6615–20.
- (26) (a) Gonzalez, C.; Schlegel, H. B. *J. Chem. Phys.* **1989**, *90*, 2154–2161. (b) Gonzalez, C.; Schlegel, H. B. *J. Phys. Chem.* **1990**, *94*, 5523–5527.
- (27) Martin, R. L.; Hay, P. J.; Pratt, L. R. *J. Phys. Chem. A* **1998**, *102*, 3565–3573.
- (28) Frisch, M. J. *Gaussian 09*, Revision A.2; Gaussian, Inc.: Wallingford, CT, U.S., 2009. The full reference is given in the Supporting Information.
- (29) Dennington, R. I.; Keith, T.; Millam, J. M.; Eppinnett, K.; Hovell, W. L.; Gilliland, R. *GaussView*, version 3.07 ed.; Semichem, Inc.: Shawnee Mission, KS, 2003.
- (30) Hall, N. E.; Smith, B. *J. Phys. Chem. A* **1998**, *102*, 4930–4938.
- (31) (a) Sayer, J. M.; Pinsky, B.; Schonbrunn, A.; Washtien, W. *J. Am. Chem. Soc.* **1974**, *96*, 7998. (b) Sayer, J. M.; Jenks, W. P. *J. Am. Chem. Soc.* **1977**, *99*, 464.
- (32) Norberg, J.; Foloppe, N.; Nilsson, L. *J. Chem. Theory. Comput.* **2005**, *1*, 986–993.
- (33) Garcia-Viloca, M.; González-Lafont, A.; Liuch, J. M. *J. Phys. Chem. A* **1997**, *101*, 3880.
- (34) Garcia-Viloca, M.; González-Lafont, A.; Liuch, J. M. *J. Am. Chem. Soc.* **1997**, *119*, 1081.
- (35) Anick, D. J. *J. Phys. Chem. A* **2003**, *107*, 1348.